Proceedings of the 7th World Congress on Momentum, Heat and Mass Transfer (MHMT'22)
~~Lisbon, Portugal~~ Virtual Conference – April 07 – 09, 2022
Paper No. ICMFHT 143
DOI: 10.11159/icmfht22.143

Bubble Growth in Saturated Pool Boiling of Water on a Smooth Surface

M. M. Mahmoud[1,2], Tassos G. Karayiannis[2]
[1]Faculty of Engineering, Zagazig University
44519, Zagazig, Egypt
mohamed.mahmoud@brunel.ac.uk, mbasuny@zu.edu.eg
[2]Centre for Energy Efficient and Sustainable Technologies
Brunel University London
UB8 3PH, London, UK
tassos.karayiannis@brunel.ac.uk

Abstract **-** Pool boiling has been investigated for many years and there are several models for the prediction of the nucleate pool boiling heat transfer. However, there are large discrepancies among these models. Most of the existing models depend on the nucleation site density and the bubble dynamics parameters, such as bubble growth rate, departure diameter and frequency. Thus, the performance of the heat transfer models can be affected by the models used for the prediction of the bubble dynamics parameters. In this paper, an experimental study was conducted to measure the bubble growth rate in saturated pool boiling of de-ionised water on a smooth copper surface at atmospheric pressure. The measurements were conducted only for the isolated bubble regime. A smooth surface was selected to avoid the uncertain effects of surface microstructure on bubble dynamics. The obtained experimental data were compared with some existing bubble growth models. The results demonstrated that bubble growth rate and departure diameter increase as wall superheat increases. The paper helps elucidate bubble dynamics and thus can contribute in understanding the performance and results given by existing mechanistic heat transfer models.

Keywords**:** pool boiling, bubble growth, heat transfer models

Nomenclature

A_P	projected area, [m^2]
c_{pl}	liquid specific heat, [J/kg K]
D	bubble diameter, [m]
D_s	diameter of heat transfer surface, [m]
f	bubble generation frequency, [1/s]
g	gravitational acceleration, [m/s^2]
h	heat transfer coefficient, [W/m^2 K]
h_{fg}	latent heat, [J/kg]
Ja	Jakob number, $\rho_l c_{pl} \Delta T_w / \rho_v h_{fg}$, [-]
k_{cu}	thermal conductivity of copper, [W/m K]
k_l	thermal conductivity of liquid, [W/m K]
L	characteristic length, [m]
Nu	Nusselt number, $Nu = hD_s/k_l$, [-]
P	pressure, [Pa]
Pr	Prandtl number, [-]
q''	heat flux, [W/m^2]
R	bubble radius, [m]
R^2	correlation coefficient, [-]
Ra	Rayleigh number, $\beta g(T_w - T_l)D_s^3/\alpha\nu$, [-]
t	time, [s]
t_g	growth time, [s]
t_{wt}	waiting time, [s]
T	temperature, [K]
T_{sat}	saturation temperature, [K]
T_l	liquid bulk temperature, [K]
T_w	boiling surface temperature, [K]
ΔT_w	Wall superheat, (T_w- T_{sat}), [K]
y	vertical distance, [m]

Greek Symbols

α	liquid thermal diffusivity, [m^2/s]
β	volumetric thermal expansion coefficient [1/K]
ρ_l	liquid density, [kg/m^3]
ρ_v	vapour density, [kg/m^3]
ν	kinematic viscosity [m^2/s]

1. Introduction

Boiling heat transfer can be encountered in a wide range of applications such as refrigeration and air conditioning systems, power generation (Rankine cycle), thermal desalination systems, food and chemical industries, cooling of high heat flux systems such as electronics and nuclear reactors. Understanding the boiling fundamentals is crucial for the development of accurate prediction models, not only for pool boiling but also for flow boiling applications. Although pool boiling has been investigated for many years, there is still a wide scatter among reported predictions of the boiling curve, i.e. heat flux versus wall superheat. Historically, the work conducted by Jakob and his research group, in the 1930s, may be the first attempt to suggest a mechanistic model based on the bubble-agitation mechanism (agitation in the liquid bulk and the boundary layer). This work is summarized in chapter 29 in the textbook by Jakob [1]. Based on this mechanism, several models have since emerged, such as the models suggested by Rohsenow [2] and Forster and Zuber [3]. The advantage of these models is simplicity and they do not need input parameters such as nucleation site density, bubble growth rate, departure size and frequency.

With the advent of 1960s, more researchers focused their efforts on the heat transfer mechanisms and suggested several mechanistic models based on studying one single bubble. The commonly suggested mechanisms included transient conduction, microlayer evaporation and latent heat (for bubble formation). Examples of these models were proposed by Han and Griffith [4] and Mikic and Rohsenow [5], who assumed that the heat transfer mechanism, in the area of bubble influence, is periodic quenching of the surface by the cold liquid that rushes down towards the nucleation site when the bubble departs the surface. At locations outside the area of bubble influence, the heat transfer mechanism was assumed to be natural convection. In literature, this quenching mechanism was originally called in reference [4] as "bulk-convection", while it was also referred to as transient conduction. This modelling approach was also called in literature "heat flux partitioning approach", i.e. the total heat flux is resulting from the summation of heat fluxes due to each separate mechanism. Other examples include the models by Yu and Cheng [6] and Zupančič et al. [7] who assumed natural convection, transient conduction and microlayer evaporation, the model by Kim and Kim [8] who assumed natural convection, transient conduction and latent heat and the model by Kumar et al. [9] who assumed natural convection, forced convection and latent heat transfer. These models require correlations for the prediction of nucleation site density, bubble departure diameter, and frequency, which are difficult to measure over a wide range of operating conditions and thus increase the challenge in the prediction of the pool boiling curve.

Bubble growth rate is one of the important variables required for studying the hydrodynamic forces during the bubble ebullition cycles and thus the prediction of bubble departure diameter and frequency. There are several models for the prediction of bubble growth rate, which can be divided into two categories: bubble growth in a *uniformly superheated liquid* (the bubble is fully surrounded by a superheated liquid layer) and bubble growth in a *non-uniform superheated liquid* (part of the bubble is surrounded by a superheated liquid layer, as is the case of growth on a heated surface in nucleate boiling -heterogeneous boiling). In both categories, researchers agreed on that there are two stages of bubble growth namely: inertia-controlled stage where the bubble radius is governed by the relation $R \propto t$ and heat diffusion-controlled growth (asymptotic growth) in which the relation between radius and time is $R \propto t^{1/2}$. The inertia-controlled growth dominates only the early stage of growth and thus it was ignored in most models. For instance, Forster and Zuber [10] assessed the inertia- and diffusion-controlled growth and reported that the hydrodynamics effects (inertia-controlled growth) are only important up to 0.1 ms, i.e. bubble growth rate is dominated by heat diffusion. Sernas and Hooper [11] measured the bubble growth rate for water boiling on a chromel strip (1.6 by 38.1 mm) and found that the inertia-controlled growth dominates only up to 0.05 ms. In the first category of bubble growth models (uniform superheat), the bubble was assumed to be a sphere and the heat was assumed to diffuse through the bubble wall radially from all directions. On the contrary, in nucleate boiling, due to the presence of a heated surface, the bubble shape may not be spherical and several models have been suggested to account for the non-uniform superheat around the bubble wall. For example, Han and Griffith [4] assumed that the bubble is covered with the wall thermal boundary layer in every ebullition cycle and it grows due to the evaporation of this layer (relaxation layer). Cooper [12] suggested a model based on the assumption that microlayer evaporation is the dominant mechanism in bubble growth especially at sub-atmospheric pressure. Van Stralen et al. [13] proposed a bubble growth model based on contribution from the relaxation layer (the thermal envelope around the bubble).

Mahmoud and Karayiannis [14] conducted a review study and a comparison between the existing bubble growth and departure models. They concluded that there is a wide scatter among the existing models of bubble growth and departure. This may explain the large discrepancy among researchers on the prediction of the nucleate pool boiling curve. Thus, there is a need for more experimental research to understand the bubble dynamics parameters. In this study, saturated pool boiling of de-ionized water on a polished copper surface was investigated at atmospheric pressure. The polished surface was selected to avoid other effects due to the surface micro-structure. The focus of the present paper is on the measurement of the bubble growth rate at atmospheric pressure. The results are compared with some existing models summarized in Table 1. Symbols are defined in the Nomenclature section.

Table 1: Bubble growth models in uniform and non-uniform superheat

Author	Model	Comment
Fritz and Ende [15]	$R = \left(2/\sqrt{\pi}\right) Ja\sqrt{\alpha t}, \qquad Ja = \frac{\rho_l C_{pl} \Delta T_w}{\rho_v h_{fg}}$	Uniform superheat
Forster and Zuber [10]	$R = \sqrt{\pi} Ja\sqrt{\alpha t}$	
Plesset and Zwick [16]	$R = \left(\sqrt{12/\pi}\right) Ja\sqrt{\alpha t}$	
Mikic et al. [17]	$R^+ = \frac{2}{3}\left[(t^+ + 1)^{3/2} - (t^+)^{\frac{3}{2}} - 1\right]$ $A = \left(\frac{2}{3}\frac{\rho_v h_{fg} \Delta T_w}{\rho_l T_{sat}}\right)^{0.5} \quad B = \sqrt{\frac{12\alpha}{\pi}} Ja \quad R^+ = \frac{RA}{B^2} \quad t^+ = \frac{tA^2}{B^2}$	
Cole and Shulman [18]	$R = 2.5 Ja^{0.75}\sqrt{\alpha t}$	Non-uniform superheat
Cooper [12]	$R = 2.5 Pr^{-0.5} Ja\sqrt{\alpha t}$	
Van Stralen et al. [13]	$R = 1.95 b Ja^*\sqrt{\alpha t}$ b: 0.794 for hemispherical bubbles and ≤ 1 for spherical bubbles $Ja^* = \frac{\rho_l C_{pl} \Delta T_w}{\rho_v h_{fg}} \exp - \left(\frac{t}{t_g}\right)^{0.5}$	
Du et al. [19]	$R = 2.1077 Ja^{0.7902}\sqrt{\alpha} t^n$ [mm], $n = 1.0012 e^{-P/0.3257} - 0.9624 e^{-\frac{P}{0.6161}} + 0.5$, P in MPa	

2. Experimental Setup

2.1. Boiling Chamber and Test Section

Figure 1a depicts the schematic drawing of the experimental facility. It consists of the following: (i) rectangular boiling chamber (250 × 250 × 300 mm) made of stainless steel with four transparent visualization windows (158 × 220 mm), (ii) two helical coil heat exchangers (one on the top side of the chamber to work as a condenser and one immersed in the liquid to work as a liquid sub-cooler), (iii) circulation chiller to supply the cooling water-glycol mixture to the condenser and the sub-cooler, (iv) test section insulation block made of Polyether Ether Ketone (PEEK) that accommodate the copper test section, see Figs. 1b and 1c, (v) immersion cartridge heater of power 1500 W to control the liquid bulk temperature and conduct liquid degassing before the test, (vi) data logger cDAQ from National Instruments, connected to a PC with Labview software to record the data, (vii) 1.5 kW DC power supply (Electro-Automatik) for supplying the heat to the test section, (viii) High-speed video camera (Phantom Miro Lab110) with NAVITAR 12X zoom lens system, (ix) two T-type thermocouples for measuring the liquid and vapour temperature and one pressure transducer (Omega, PX319, 0 – 3.5 bar) for measuring the system pressure.

The test section was made of oxygen-free copper and was insulated with a PEEK housing as seen in the exploded view in Fig. 1b and the assembly drawing in Fig. 1c. The copper test piece has a diameter of 30 mm and a height of 42.5 mm. It has five holes of diameter 0.6 mm at 6 mm equal distance along the vertical centreline to insert five thermocouples, and an O-ring shoulder of size 2.5 mm width and 2 mm depth leaving 25 mm diameter as a boiling surface, see Fig. 2b. The test piece was connected to a copper heater block using M10 thread connector (made of copper) and the thermal contact resistance was reduced by a thermal paste, see Fig. 2a for the assembly of the test section and the heater block. The heater block has

four vertical holes (see Fig. 2c) with diameter 12 mm to accommodate four cartridge heaters (400 W each), which are connected to the DC power supply. The test section was manufactured using High Precision Micro Milling Machine (HERMLE C20U) and the boiling surface was finished by diamond turning machine to obtain a smooth surface. The surface was analysed using Surface Metrology System (NP FLEX-3D) and the S_a value of the tested surface was 49.6 nm. The temperature reading of the five vertical thermocouples was plotted versus the vertical distance and the gradient was used to calculate the applied flux q'' using Eq. (1). The measured temperature versus distance exhibited linear fitting with a correlation coefficient, $R^2 > 0.97$, which verifies the 1D assumption in calculating q''. The temperature difference between the wall and the saturation temperature (wall superheat) was calculated using Eq. (2).

$$q'' = -k_{cu}\frac{dT}{dy} \tag{1}$$

$$\Delta T_w = T_w - T_{sat} \tag{2}$$

The saturation temperature was based on the pressure measured using the pressure transducer. All thermocouples were calibrated and the maximum uncertainty in the temperature measurements was ± 0.5 K. The propagated uncertainty analysis was calculated according to the method given in Coleman and Steel [20]. The highest uncertainty in the heat flux was 7 %.

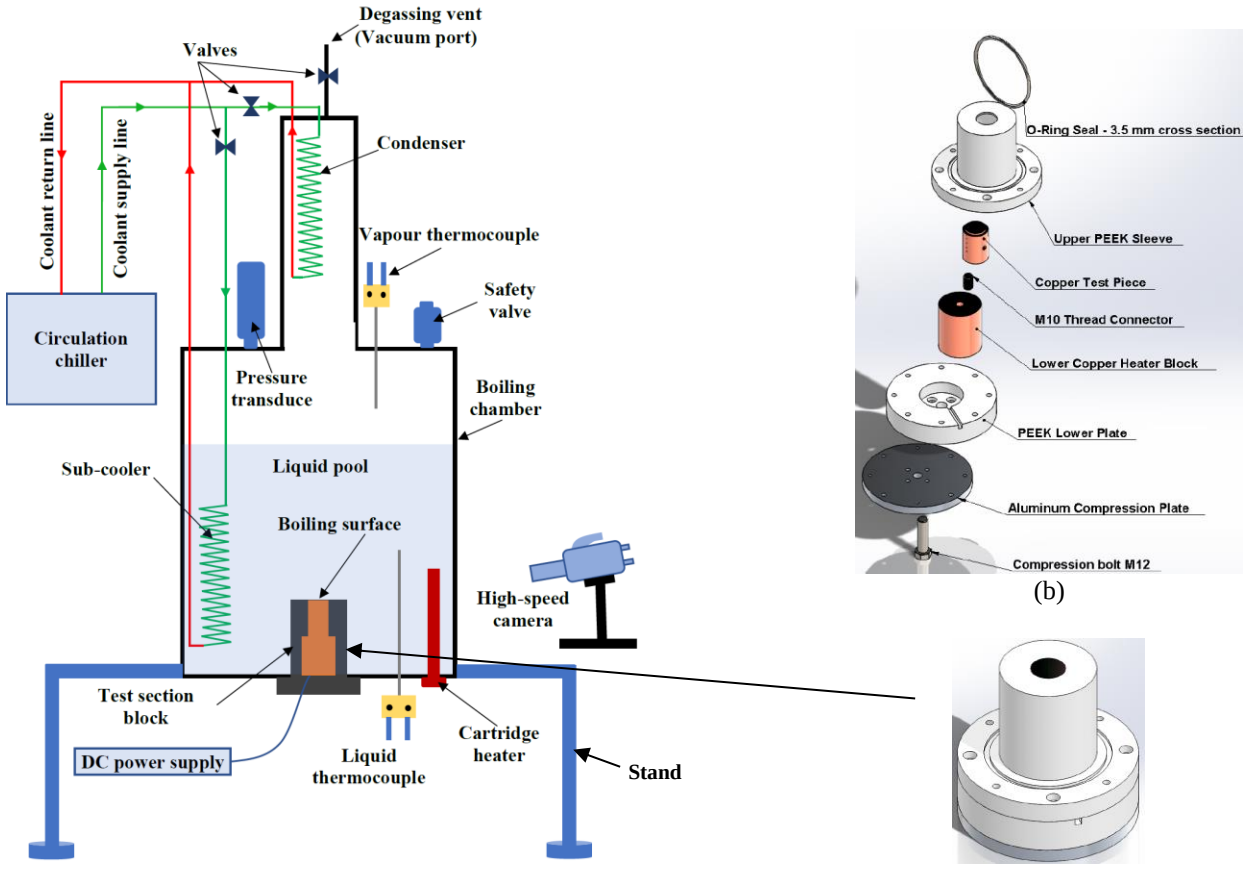

Fig. 1: (a) Schematic drawing of the experimental facility, (b) Exploded view of the test section, and (c) The test section assembly

2.2. Experimental Validation

Many researchers validated their experimental system by conducting boiling experiments and comparing the experimental boiling curve with the well-known Rohsenow [2] pool boiling correlation. This approach may not be accurate because boiling depends strongly on the surface microstructure. In the present study, experimental system

validation was conducted using natural convection single-phase experiments rather than boiling experiments. Fig. 3 depicts the heat flux plotted versus the temperature difference between the surface (T_w) and the liquid (T_L). The results were compared with the natural convection correlation reported in Bergman et al. [21], see Eq. (3). It is obvious that there is a good agreement between the measurements and the prediction with average deviation of 8.8 %, which verifies the accuracy of the experimental measurement system.

$$Nu = \begin{cases} 0.54Ra^{1/4} & 10^4 \le Ra < 10^7, \quad Pr > 0.7 \\ 0.15Ra^{1/3} & 10^7 \le Ra < 10^{11}, \quad all\ Pr \end{cases} \tag{3}$$

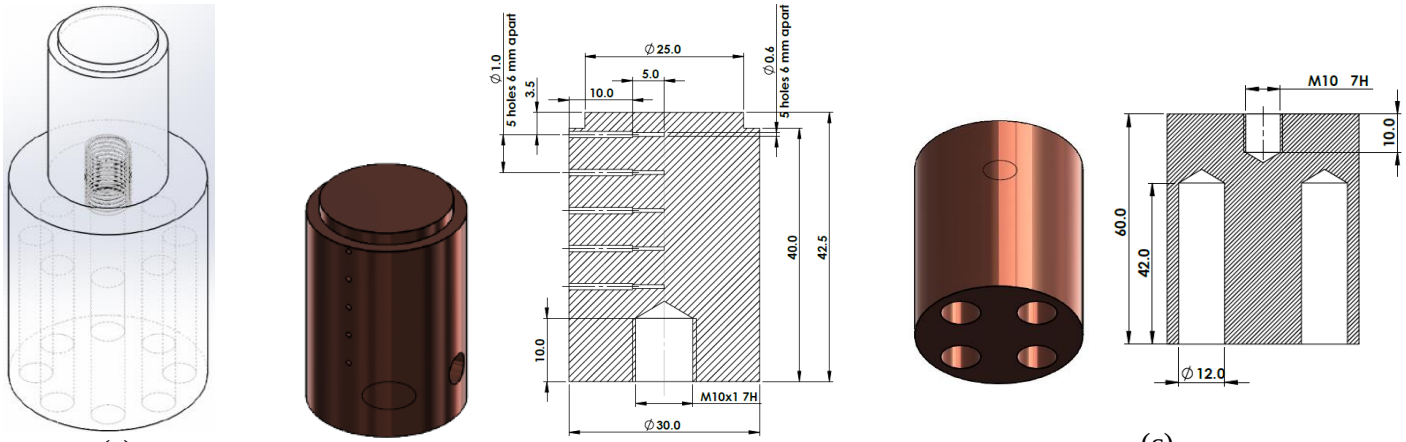

(a) (b) (c)

Fig. 2: (a) Copper test section and the heater block, (b) Test section, and (c) The heater block

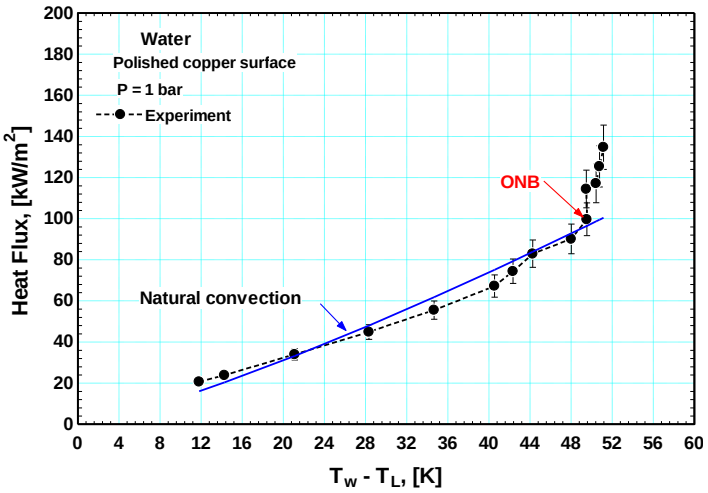

Fig. 3: Experimental validation using single-phase natural convection

3. Results and Discussion

This section presents the measured bubble growth rate in the isolated bubble regime for wall superheat of 2.6 K, 5.3 K and 8.3 K. The Phantom high-speed camera was used for recording the videos at resolution of 1024 × 768 pixel and speed 2182 f/s. All bubble size measurements were conducted using ImageJ software. The measured bubble diameter was the equivalent diameter calculated from the projected area of the bubble shape (the shape is not always spherical) as defined by Eq. (4). It is worth mentioning that the camera was tilted with an angle of 17^0, which will make the size of the measured object smaller than the real size. To consider the effect of the tilt angle, the camera was calibrated at the aforementioned

settings (resolution, speed and angle) using a standard ball bearing of 12.7 mm diameter, which was measured using a micrometer screw gauge. The measured equivalent diameter using the projected area was found to be 8.9 mm (29.9 % less than the real size). Thus, the measured diameter in the present study must be corrected by multiplying the measured value by 1.299. In fact, the camera tilting affects only the measured vertical side not the horizontal side. This was also confirmed by measuring the height of a standard object of (height 14.74 mm) at the same camera settings and tilting angle and the measured value was 13.1 mm (11.1 % lower than the real height). Thus, the effect of camera tilt on an object height is much smaller than the effect on the projected area. The effect of camera tilt on the vertical height is already included in the projected area and thus no need for correction.

$$D = \sqrt{\frac{4A_P}{\pi}} \tag{4}$$

It is well-known that there is a random distribution of nucleation sites on a surface with a random microstructure. In the present study, measurements were conducted for a selected active nucleation site, in the isolated bubble regime, as seen in the pictures of Fig. 4a. The measurements were conducted for bubbles without horizontal or vertical coalescence. Fig. 4b depicts the effect of superheat on the measured bubble diameter versus time at atmospheric pressure in saturated boiling of de-ionized water. It is obvious that, for the lowest degree of superheat, the bubble grows rapidly for a short time (< 4 ms) then it grows very slowly until it departs after 33.9 ms (growth time, t_g) with departure diameter 1.4 mm. The measured waiting time (t_{wt}) for this bubble was 2.3 ms, which gives departure frequency of ($f = 1/(t_g + t_{wt})$) of about 28 Hz. Increasing the superheat to 5.3 and 8.3 K resulted in the same trend but with a higher rate, lower growth time and larger departure diameter. For superheat 5.3 K, the growth time was 9.6 ms, the waiting time was 0.92 ms ($f \approx 95\ Hz$) and the departure diameter was 1.9 mm while for superheat 8.3 K the growth time was 11 ms, waiting time 0.46 ms ($f \approx 115\ Hz$) and the departure diameter was 2.8 mm. It is obvious that the departure diameter increased from 1.4 to 2.8 mm when the superheat increased from 2.6 to 8.3 K.

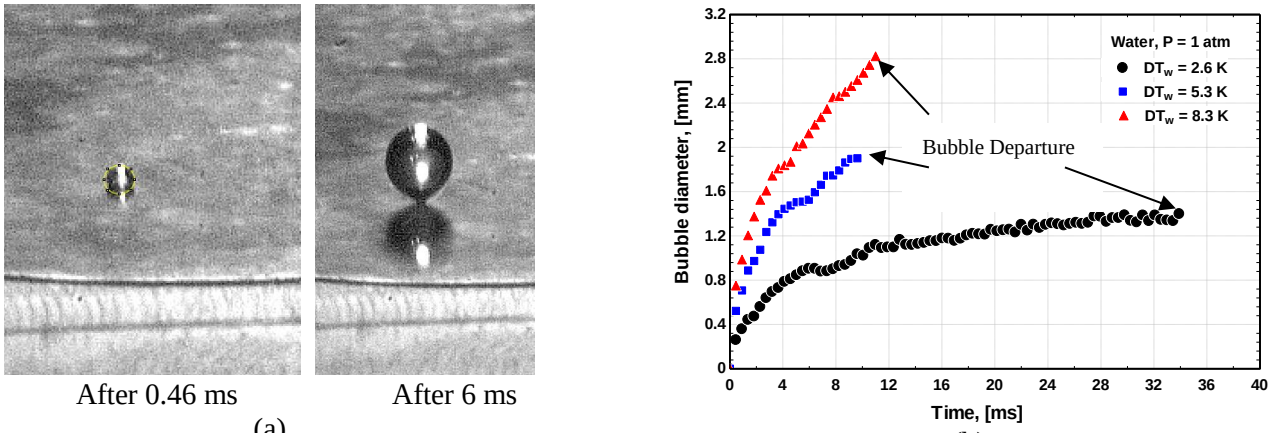

Fig. 4: (a) Pictures of bubble growth at 8.3 K superheat, (b) effect of superheat on bubble growth diameter versus time.

Fig. 5 illustrates the comparison between the measured bubble growth rate and the models summarized in Table 1. The comparison demonstrated that the model by Fritz and Ende [15] and Cole and Shulman [18] and Van Stralen et al. [13] under-predict the bubble growth significantly, while the models by Forster and Zuber [10], Plesset and Zwick [16], Mikic et al. [17], Cooper [12] and Du et al. [19] predict the experimental data reasonably well, especially for superheat 5.3 and 8.3 K. For the lowest superheat, most correlations could not predict the experimental trend because these models were based on the relation $D \propto t^{0.5}$ while the best fit for the experimental data at the lowest superheat is $D \propto t^{0.3}$. This means that the existing models may not be valid at low superheats (< 5.3 K) or Ja < 15. It is interesting to note that most researchers did not account for the camera tilting angle, which could result in different conclusions about the performance of the existing models. For example, if the effect of camera tilt was ignored in the present study, all the above models that agreed with the data will over-predict the data. On the contrary, the model by Fritz and Ende [15], which under-predicted the data will agree with the experimental data.

Fig. 5 (i) depicts a comparison between the data of the present study and the experimental data from [22, 23] for saturated boiling of water at nearly the same superheat but different substrate materials. Gerardi et al. [22] studied saturated boiling of water on a sapphire substrate (thermal conductivity 25.1 W/m K) with the boiling side coated with Indium Tin Oxide (ITO) while Kangude and Srivastava [23] used the same approach but with borofloat glass (thermal conductivity 1.1 W/m K) as the substrate material. In the study by Gerardi et al. [22], the bubble growth rate, growth time and departure diameter were larger than the values of the present study. The growth time and departure diameter were 51.5 % and 15.8 % larger, respectively. On the contrary, in the study by Kangude and Srivastava [23], the growth rate was lower, the growth time was extremely larger and the departure diameter was nearly the same compared to this present study. The growth time was 2494.5 times larger while the departure diameter was larger by 5.3 %. They attributed this large growth time to the hydrophobicity of the surface (the measured contact angle in their study was 90^0). It is worth mentioning that the measured contact angle in the present study on the copper surface was 85^0. It is also interesting to note that the two studies by [22] and [23] are similar in that boiling occurred on the ITO heater side but the results are completely different. The reason is not understood, i.e. is the difference due to the effect of substrate material or due to other factors. These discrepancies and uncertainty increase the research challenge in this area and raise the question about the validity of bubble growth measured on glass or other transparent substrates in relation to metallic surfaces of practical interest.

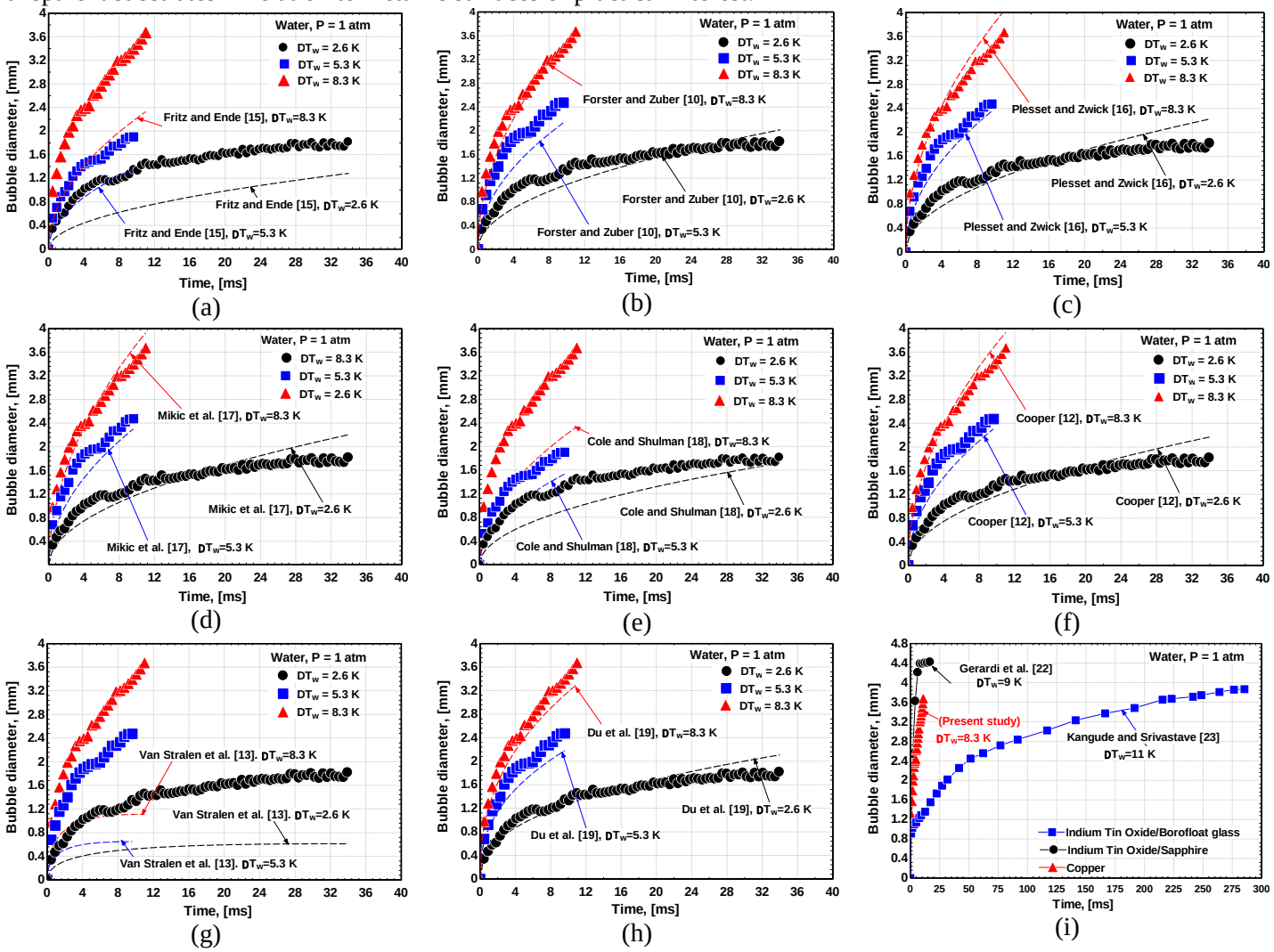

Fig. 5: Comparison of the bubble growth models (a-d: uniform and e-h: non-uniform superheated layer) and past experiments (i) with the present results for bubble growth.

4. Conclusion

Bubble growth was measured in saturated boiling of water on a smooth copper surface to help understand the bubble dynamics parameters required for the development of mechanistic heat transfer models. The results were compared with some existing models for bubble growth in uniform and non-uniform superheat. It was concluded that the models by Forster and Zuber [10], Plesset and Zwick [16], Mikic et al. [17], Cooper [12] and Du et al. [19] predicted the experimental data reasonably well. The effect of camera tilting angle may result in different conclusions among researchers. Additionally, due to the fact that glass substrates with transparent heating may not represent the real metallic boiling surfaces, more experiments are required to measure the bubble dynamics on metallic surfaces over a wide range of operating conditions and fluids.

Acknowledgements

The work was carried out with the support of the Engineering and Physical Sciences Research Council of the UK, under Grant: EP/S019502/1.

References

[1] M. Jakob, "*Heat Transfer"*, vol. 1, New York, NY Wiley 1949.

[2] W. M. Rohsenow, "A method of correlating heat transfer data for surface boiling of liquids", Technical Report No. 5, Massachusetts Institute of Technology, *M. I. T. Division of Industrial Corporation*, Cambridge, Massachusetts, 1951.

[3] H. K. Forster and N. Zuber, "Dynamics of vapor bubbles and boiling heat transfer", *AIChE Journal*, vol. 1, no. 4, pp. 531 – 535, 1955.

[4] C-Y. Han and P. Griffith, "The mechanism of heat transfer in nucleate pool boiling-Part II the heat flux-temperature difference relation", *Int. J. Heat Mass Transfer*, vol. 8, pp. 905 – 914, 1965.

[5] B. B. Mikic and W. M. Rohsenow, "A new correlation of pool boiling data including the effect of heating surface characteristics", *Heat Transfer Engineering, ASME*, May, pp. 245 – 250, 1969.

[6] B. Yu and P. Cheng, "A fractal model for nucleate pool boiling heat transfer, *Heat Transfer Engineering, ASME*, December, vol. 124, pp. 1117 – 1124, 2002.

[7] M. Zupančič, P. Gregorčič, M. Bucci, C. Wang, G. M. Aguiar, M. Bucci, "The wall heat flux partitioning during the pool boiling of water on thin metallic foils", *Appl. Therm. Eng.*, vol. 200, pp.117638, 2022.

[8] M. Kim and S. J. Kim, "A mechanistic model for nucleate pool boiling including the effect of bubble coalescence on area fractions", *Int. J. Heat Mass Transfer*, vol. 163, pp. 120453, 2020.

[9] A. Kumar, A. K. Behura, D. K. Rajak, R. Kumar, M. H. Ahmadi, M. Sharifpur, O. Bamisile, "Performance of heat transfer mechanism in nucleate pool boiling-a relative approach of contribution to various heat transfer components", *Case Studies in Thermal Eng.*, vol. 24, pp. 100827, 2021.

[10] H. K. Forster and N, Zuber, "Growth of a vapour bubble in a superheated liquid", *J. of Applied Physics*, vol. 25, no. 4, pp. 474 – 478, 1954.

[11] V. Sernas and F. C. Hooper, "The initial vapor bubble growth on a heated wall during nucleate boiling", *Int. J. Heat Mass Transfer*, vol. 12, no. 12, pp. 1627 – 1630, 1969.

[12] M. G. Cooper, "The microlayer and bubble growth in nucleate pool boiling", *Int. J. Heat Mass Transfer*, vol. 12, pp. 915 – 933, 1969.

[13] S. J. D. van Stralen, M. S. Sohal, R. Cole, W. M. Sluyter, "Bubble growth rate in pure and binary systems: combined effect of relaxation and evaporation microlayers", *Int. J. Heat Mass Transfer*, vol. 18, pp. 453 – 467, 1975.

[14] M. M. Mahmoud and T. G. Karayiannis, "Pool boiling review – Part I: fundamental of boiling and relation to surface design", *Thermal Science and Engineering Progress*, vol. 25, 2021.

[15] W. Fritz and W. Ende, "Über den verdampfungsvorgang nach kinematographischen aufnahmen an dampfblasen", *Phys. Zeitschr*. 37, pp. 391 – 401, 1936.

[16] M. S. Plesset and S. A. Zwick, "The growth of vapour bubbles in superheated liquids", *J. of Applied Physics*, vol. 25, no. 4, pp. 493 – 500, 1954.

[17] B. B. Mikic, W. M. Rohsenow, P. Griffith, "On bubble growth rates", *Int. J. Heat Mass Transfer*, vol. 13, pp. 657 – 666, 1970.

[18] R. Cole and H. I. Shulman, "Bubble growth rates at high Jakob numbers", *Int. J. Heat Mass Transfer*, vol. 9, pp. 1377 – 1390, 1966.
[19] J. Du, C. Zhao, H. Bo, "A modified model for bubble growth rate and bubble departure diameter in nucleate pool boiling covering a wide range of pressure", *Appl. Therm. Eng.* 145, pp. 407 – 415, 2018.
[20] H. W. Coleman and W. G. Steele, "*Experimentation, validation, and uncertainty analysis for engineers*", John Willey and Sons Inc., NJ, USA, 3rd ed., 2009.
[21] T. L. Bergman, A. S. Lavine, F. P. Incropera, D. P. Dwitt, "*Fundamentals of heat and mass transfer*", John Willey and Sons Inc., NJ, USA, 7th ed., 2011.
[22] C. Gerardi, J. Buongiorno, L-W. Hu, T. Mckrell, "Study of bubble growth in water pool boiling through synchronized infrared thermometry and high-speed video", *Int. J. Heat Mass Transfer*, vol. 53, pp. 4185 – 4192, 2010.
[23] P. Kangude and A. Srivastava, "Understanding the growth mechanism of single vapor bubble on a hydrophobic surface: experiments under nucleate pool boiling regime", *Int. J. Heat Mass Transfer*, vol. 154, pp. 119775, 2020.